crater, or any post-crater resurfacing history. In this fashion, crater counts can be performed that confidently date superposed mantle surfaces as well as un-mantled ejecta deposits, which can constrain the emplacement history of the mantle.

3. Methods

Young craters were identified at various latitudes based on their geomorphic characteristics using THEMIS (Christensen et al., 2004), CTX (Malin et al., 2007), and HiRISE data (McEwen et al., 2007). All of the craters examined in this study are simple impact craters, ranging in diameter from 0.8 to 7.3 km (Table 1). Pristine craters this size are bowl-shaped with a crisp raised rim crest and distinct ejecta deposits (e.g., Strom and Croft, 1992). Ejecta may vary in morphology (e.g., Barlow and Bradley, 1990), but typically the continuous ejecta deposit is well-defined. At the highest latitudes where polygonally patterned ground is pervasive, the comparative distinctness of rim crests was used to distinguish young craters. Not all of these young craters exhibit rays in nighttime thermal infrared (nTIR) data. Thirteen craters imaged by HiRISE and located in the southern hemisphere were selected for this study, and for comparison, three rayed craters (identified by Tornabene et al., 2006) in the northern hemisphere. Locations of these craters and summary data are presented in Fig. 1 and Table 1. Crater counts were conducted exclusively on sub-meter resolution HiRISE data (McEwen et al., 2007). For each count a 100 m grid was implemented using Hawth's tools (Beyer, 2004) to facilitate an exhaustive search of near-rim ejecta deposit terrain for superposed craters. The CraterTools ArcMap extension (Kneissl et al., 2011) was used to consistently measure crater diameters without distortion. All crater data is presented in the incremental-plot style of Hartmann with isochrons from Hartmann (2005).

4. Crater count data

Presentation of the crater count data is organized geographically. First, the three rayed craters in the equatorial region are considered (Figs. 2–4). These craters are located far from regions of latitude-dependent mantling (Fig. 1). Second, two high latitude craters are discussed (Figs. 5 and 6), which have pervasive polygonally patterned ground draping their interiors, near-rim

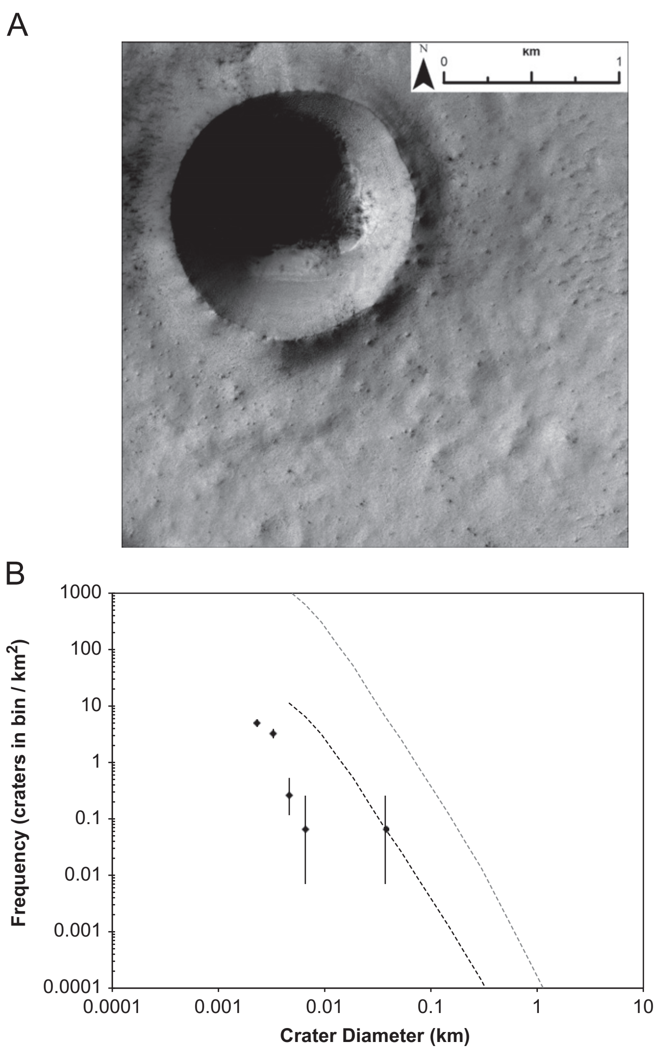

Fig. 6. (A) An unnamed 1.4-km diameter crater is found in Sisyphi Planum (77.9°S, 345.4°E). Polygonally patterned ground is found pervasively on the crater floor, wall, and rim, and on surrounding terrain. Portion of HiRISE: ESP_013968_1020. (B) A crater count revealed 332 craters on 15.1 km^2 of near-rim deposits surrounding the unnamed crater (77.9°S, 345.4°E). Isochrons of Hartmann (2005) indicate a best-fit age of 0.3 Ma. The grey dashed line marks the Early Amazonian boundary of Hartmann (2005).

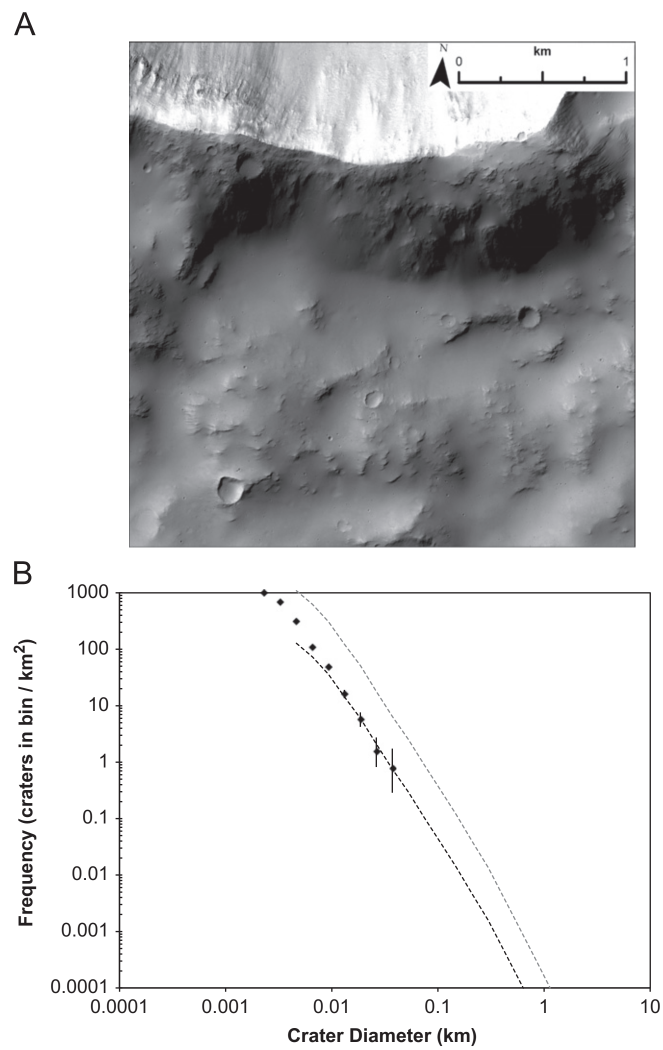

Fig. 7. (A) An unnamed 7.3-km diameter crater is found in Terra Cimmeria (20.8°S, 150.6°E). No evidence of latitude-dependent mantling is observed. Portion of HiRISE: PSP_010032_1590. (B) A crater count revealed 12,482 craters on 3.8 km^2 of near-rim deposits surrounding the unnamed crater (20.8°S, 150.6°E). Isochrons of Hartmann (2005) indicate a best-fit age of 31.5 Ma. The grey dashed line marks the Early Amazonian boundary of Hartmann (2005).